Contrib Mineral Petrol (1996) 126:152–168 © Springer-Verlag 1996

S. Inger · W. Ramsbotham · R. A. Cliff · D. C. Rex

Metamorphic evolution of the Sesia-Lanzo Zone, Western Alps: time constraints from multi-system geochronology

Received: 12 October 1995/Accepted:25 June 1996

Abstract The Sesia-Lanzo Zone is a polymetamorphic unit containing Hercynian granulite relics overprinted by eclogite and greenschist facies metamorphism and deformation during the Alpine orogeny. Different parts of the unit record different stages on the *P-T*-deformation evolution, allowing multi-system isotopic studies to unravel the precise timing of the metamorphic history. New Rb–Sr white mica and U–Pb sphene data constrain the age of eclogite facies metamorphism and deformation to 60–70 Ma. This substantially alters the common view of early- to mid-Cretaceous eclogite facies metamorphism in this unit. The new results are more consistent with the established geotectonic framework for the Alpine orogeny, since they do not require a prolonged period of depressed geothermal gradient at a time when the region was in extension. It is also more concordant with recent studies of other units that demonstrate post-Cretaceous high-pressure metamorphism. Step-heated ^{40}Ar–^{39}Ar analysis of phengites yields good plateaux giving ages older than the corresponding Rb–Sr age. Such anomalously high ages indicate the presence of radiogenic argon-rich fluids in the grain boundary network under the fluid/pressure conditions acting during this high-pressure metamorphic event. The U–Pb sphene ages are variable in polymetamorphic rocks, and show inheritance of older Pb or sphene crystals into the high-pressure event. Two monometamorphic assemblages yield concordant ages at 66 ± 1 Ma, reflecting crystallisation of the eclogite facies assemblage. The Gneiss Minuti Complex (GMC) lies structurally below the Eclogitic Micaschists, and its pervasive greenschist facies fabric yields tightly clustered Rb–Sr white mica ages at 38–39 Ma. This greenschist event did not affect the majority of the EMC. The ^{40}Ar–^{39}Ar ages of micas formed at this time were very disturbed, whereas micas surviving from an earlier higher pressure assemblage had their ^{40}Ar–^{39}Ar system reset. The greenschist event did not strongly affect U–Pb systematics in Hercynian age sphenes, suggesting that the GMC did not uniformly suffer an eclogite facies metamorphism during the Alpine cycle, but was juxtaposed against the EMC later in the orogeny. This model still requires that the locus of deformation and metamorphism (and possibly fluid flux) moved outboard with time, leaving the Sesia-Lanzo basement as a shear-bounded unreactive block within the orogenic wedge.

S. Inger (✉) · W. Ramsbotham[1] · R. A. Cliff · D. C. Rex
Department of Earth Sciences, University of Leeds, Leeds, LS2 9JT, UK

[1]Deceased

Editorial responsibility: I. Parsons

Introduction

Understanding the geodynamics of high-pressure metamorphic terrains is an important goal in the study of orogenic processes, offering insights into the mechanical and thermal behaviour of the lithosphere. High-pressure metamorphic assemblages are common in rocks of oceanic affinity that have been exhumed from fossil subduction zones, and although the mechanisms of exhumation are not well understood, the driving force behind their deep burial is clear. More problems arise in continental crust that preserves a high-pressure history because it is difficult to envisage how such buoyant material can be subducted to the depths required to stabilise eclogite assemblages. Moreover, doubts are often expressed about the thermal regime in which such material could be returned to the surface at sufficient speeds to escape retrogression (Ernst 1975; Rubie 1984). The timing of key points in the metamorphic and tectonic evolution of such units is therefore an important constraint on the geodynamics of

eclogite metamorphism. Unfortunately, many geochronological studies of eclogite terrains have been hindered by disequilibrium effects and partial retrogression, to the extent that even the age of the metamorphic peak is rarely known with the precision necessary for studying tectonic processes in young mountain belts.

Eclogite metamorphism is recorded in several units of the European Alps. These units are particularly important in understanding the dynamics of the Alpine orogeny because the available timescale for the collision, burial and exhumation cycle is known to be less than 100Ma. This study focuses on the Sesia-Lanzo Zone, an extensive unit of eclogite-bearing continental crust with affinity to the African continent prior to the Eocene collision with Europe. Its metamorphic history is quite well constrained, but the timing of key points on its pressure-temperature evolution is more controversial (Compagnoni et al. 1977; Oberhänsli et al. 1985). The Zone contains a wide variety of lithologies preserving different parts of the pressure-temperature and deformation history, offering the potential for multi-system isotopic dating of key episodes in this history. In addition to direct tectonic constraints, this approach can yield information on the behaviour of geochronometric systems during the metamorphic cycle which does not become apparent when dealing with a single mineral/isotope system, which may be subject to special controls in the high-pressure environment.

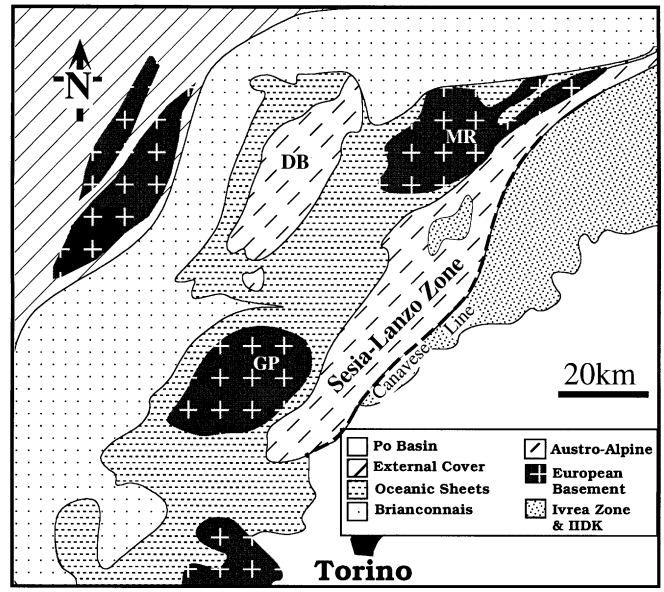

Fig. 1 Tectonic units of the Western Alps (*GP* Gran Paradisio, *DB* Dente Blanche, *MR* Monte Rosa)

Geological setting

The Sesia-Lanzo Zone (SLZ) crops out over approximately 1200 km^2 in the Italian Western Alps (Fig. 1). It has been divided into two major tectonic elements (Fig. 2). The uppermost element is known generally as the Seconda Zona Diorito-Kinzigitica (IIDK) (Williams and Compagnoni 1983), and is mostly composed of Hercynian metamorphic rocks that have suffered limited thermal effects of the Alpine orogeny. This unit will not be considered further here. The lower element is a complex of metamorphosed sediments and igneous rocks that mostly represent Austro-Alpine continental crust of the African-Adriatic plate. Different parts of this element record different stages in the Alpine tectonic and metamorphic evolution (Compagnoni 1977; Compagnoni et al. 1977; Lardeaux and Spalla 1991). The upper unit is known as the Eclogitic Micaschist Complex (EMC), comprising metasedimentary and metaigneous rocks that preserve eclogite facies assemblages overprinting relic amphibolite-granulite Hercynian assemblages (Fig. 3). Recent mapping by Italian and Swiss geologists (Venturini et al. 1991, 1994) has identified a sub-unit of the EMC that retains no amphibolite-granulite metamorphic relics, and has lithological affinities with European margin cover sequences of the Combin Zone. It is likely that these rocks therefore entered the Alpine orogenic cycle as sediments and have no Hercynian history. The recognition of units that may not have a pre-Alpine metamorphic record offers important targets for new sampling because they avoid the effects of inherited isotope signals.

The lowermost, eastern sector of the Sesia-Lanzo Zone is the Gneiss Minuti Complex (GMC), a series of metamorphic rocks, dominantly metaigneous, that record a pervasive greenschist facies metamorphism. Between these units is a narrow *transition zone* where EMC assemblages are partially overprinted by the greenschist facies episode. In addition to this general lithotectonic stratigraphy,

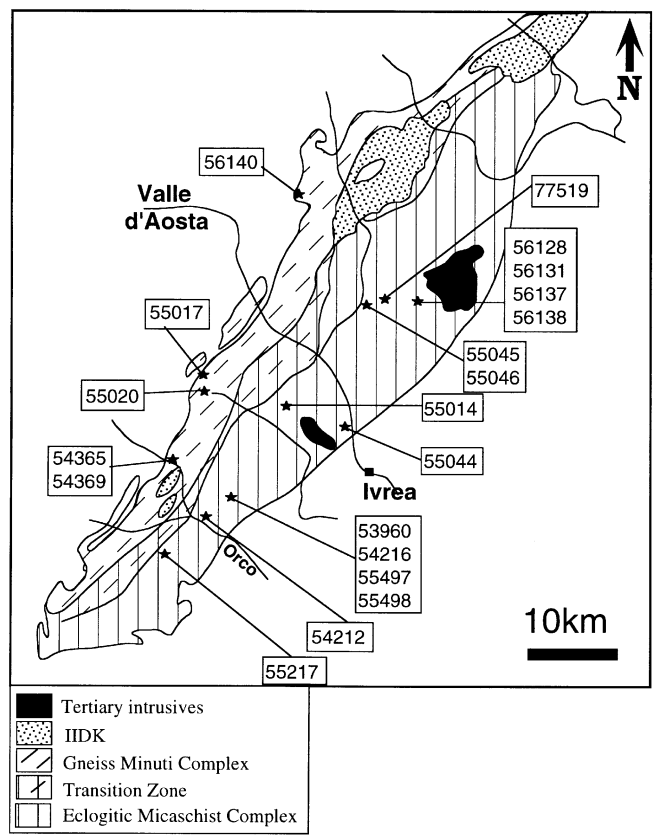

Fig. 2 Geology of the Sesia-Lanzo Zone showing sample localities; after Compagnoni (1977)

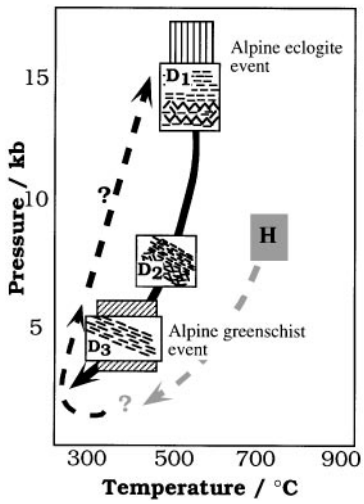

Fig. 3 Summary *P-T*-d evolution of the Sesia-Lanzo Zone, showing Variscan high-grade history (*grey*, *H*), Alpine eclogite-facies phase (*vertical ornament*) and Alpine greenschist facies phase (*diagonal ornament*). Deformation phases are those referred to in text

there are along-strike variations in the recorded metamorphic history at similar levels (Compagnoni et al. 1977).

Deformation recorded in the SLZ also varies throughout the zone. Fabrics and structures in the EMC formed under high-pressure conditions – the metamorphic foliation is defined by high-pressure phengites and post-dates the occasional relic Hercynian granulite banding. The foliation is folded but not pervasively transposed, suggesting that it underwent no penetrative deformation at later points on the pressure-temperature history than the eclogite stage. Fabrics within the Gneiss Minuti Complex, by contrast, are ubiquitously defined by greenschist facies minerals suggesting penetrative syn-tectonic recrystallisation. Relict high-pressure phases have been reported in rocks that are now assigned to the GMC, implying that the whole of the Sesia-Lanzo Zone acted as a mechanically contiguous unit throughout its post-eclogite Alpine metamorphic history (Pognante et al. 1987; Ridley 1989).

Metamorphic history

The polymetamorphic history of the SLZ, together with a dearth of low-variance assemblages, has hindered the estimation of metamorphic conditions prevailing during the Alpine cycle. After amphibolite/granulite facies conditions in the Hercynian, the early Alpine high-pressure metamorphism recorded in the EMC resulted from pressures in excess of 15 kbar, possibly as high as 20 kbar, and temperatures of $550 \pm 50\,^{\circ}C$ (Compagnoni et al. 1977; Williams and Compagnoni 1983; Pognante et al. 1987). The Alpine greenschist metamorphism occurred at temperatures closer to 450–500 °C, and pressures lower than 13 kbar (Williams and Compagnoni 1983; Pognante et al. 1987; Pognante 1989). Although the relationship between metamorphic conditions and deformation phases vary slightly depending upon locality, in this study, dealing mainly with samples from the central and southern parts of the SLZ, the metamorphism can be related to deformation in the following general sequence (Ramsbotham et al. 1994):

D_o/M_o. Amphibolite to granulite assemblages and fabrics now preserved as relics in EMC units.

D_1/M_1. High-pressure planar fabrics (T_E), formed in a regime of general non-coaxial shear with top-east vorticity. Later stages of this deformation generated crenulation cleavages (T_{cc}).

D_{1b}/M_{1b}. Partly transpositional sub-vertical cleavage developed under retrograde (blueschist) conditions.

D_2. In the transitional zone, where high-pressure assemblages have been partially overprinted by greenschist facies minerals, T_E fabrics are rotated into parallelism with T_G fabrics (below). This may therefore be linked to D_3 but may post-date it.

D_3/M_3. In the Gneiss Minuti Complex, a thorough recrystallisation under greenschist facies conditions was associated with formation of a penetrative planar fabric (T_G) whose kinematics are uncertain. These fabrics do not extend into the EMC.

Note that these D/M annotations are used to relate *only* to the local history and should not be correlated with the same numbers used by other authors. Controversies stem from the relationships between the EMC and GMC. Williams and Compagnoni (1983) and Paschier et al. (1981) asserted that the two units had different early metamorphic histories and were juxtaposed by thrusting after the peak of the high-pressure metamorphism, whereas Pognante et al. (1987) and Ridley (1989) suggested that the units have remained mechanically contiguous since early-Alpine times, and the difference in metamorphic record represents a shift in the locus of metamorphic and tectonic recrystallisation, possibly engendered by fluid flow. Isotopic dating of metamorphic histories may offer important additional data to discriminate between such models.

Geochronology

The age of high-pressure metamorphism in the Sesia-Lanzo Zone is often cited as "130–85 Ma," (Hunziker et al. 1989) reflecting the poor resolution of dating techniques that have been applied. Oberhänsli et al. (1985) presented the first detailed geochronological investigation of the SLZ high-pressure metamorphism, based on samples from the environs of the Monte Mucrone metagranitoid. They concluded that the high-pressure peak occurred at 129 ± 15 Ma, the age yielded by a whole-rock Rb-Sr isochron from the metagranitoid. Subsequent ages yielded by the K–Ar, Rb–Sr and Ar–Ar techniques were attributed to post-metamorphic cooling. Their garnet Rb–Sr mineral isochron age of 113 Ma may be suspect because of the unusually high Rb/Sr ratio in the garnet suggesting that the inheritence of radiogenic phases is controlling the Sr isotopic composition. Stöckhert et al. (1986) presented

K–Ar data on phengites and suggested that the EMC cooled through the closure temperature of 350 °C at around 80 Ma.

A re-evaluation of the age of high-pressure metamorphism in the Sesia Zone is timely for several reasons. Firstly, K–Ar and Ar–Ar data must be re-assessed in the light of recent work that demonstrates a highly heterogeneous and *largely undetectable* distribution of excess argon in rocks from the Sesia Zone in particular, and in high-pressure terrains in general (Arnaud and Kelley 1995; Kelley et al. 1993; Ruffet et al. 1995; Reddy et al. in press). In addition, incomplete resetting of granite whole-rock Rb–Sr isochrons during cooling, metamorphism and recrystallisation has been demonstrated in a number of polymetamorphic terrains, and a single isochron from Monte Mucrone may not necessarily reflect a well-defined metamorphic or tectonic event (Kwan et al. 1992; Marquer and Peucat 1994). Secondly, many recent geochronological studies of Alpine high-pressure metamorphism indicate that high-pressure conditions continued into the middle Tertiary rather than the conventionally accepted "Cretaceous."(Tilton et al. 1991; Becker 1993; Bowtell et al. 1994) The present study concentrates on the Rb–Sr technique on white micas, which does not suffer the problems of excess radiogenic component to which the Ar–Ar and particularly K–Ar techniques are prone. The ^{40}Ar–^{39}Ar data are presented to show that they deviate from the behaviour predicted by conventional closure temperatures, bolstering our assertion that studies in the EMC based only on this system should be evaluated more cautiously.

We have also dated sphene from calcareous lithologies using the U–Pb technique. This mineral has a closure temperature higher than the Alpine thermal peak (Mezger et al. 1991), so if it crystallised as part of the high-pressure assemblage it should yield the age of that crystallisation event.

Analytical techniques

Samples were crushed and sieved, and minerals separated by standard magnetic and heavy liquid methods. Micas were separated by adherence to paper, which usually gave a concentration of better than 99%. Where impurities were not quartz, separates were further purified by hand picking. Carbonate was removed from silicate splits by washing in dilute acetic acid and water. Pyroxenes, epidotes and sphenes were all hand picked. Mineral separates were washed in an ultrasound bath with three aliquots each of methanol and sub-boiling distilled water. Samples for U–Pb analysis were further acid washed with 6 M HCl and water. Mixed spikes (^{84}Sr–^{87}Rb and ^{202}Pb–^{233}U–^{236}U) were used and standard ion-exchange procedures were followed. The Rb, U and Pb measurements were performed on the VG Micromass 30 mass spectrometer at the University of Leeds.

Lead isotopes were corrected for fractionation by comparison with the NBS-981 standard, and for blank by analysis of a total procedural blank with each batch of 5 samples. The U–Pb measurements utilised a mixed ^{202}Pb–^{233}U–^{236}U spike whose U/Pb ratio was determined by analyses of SRM 612 trace element glass, and checked against a standard zircon solution and a mixed gravimetric solution kindly provided by the late J.C. Roddick. The standard error of the mean of these analyses suggests the U/Pb ratio of the spike is known to within $\pm$ 0.25%. Strontium was analysed on the VG Isomass 54E at Leeds, corrected by reference to the NBS-987 standard whose measured $^{87}Sr/^{86}Sr$ averaged 0.710300 $\pm$ 0.000022 (187 runs) throughout this study and whose "true" value was taken as 0.71024. Errors in $^{87}Sr/^{86}Sr$ and $^{87}Rb/^{86}Sr$ were assessed by replicate analysis of homogeneous natural mica samples, which yielded 2-sigma reproducibility of 0.005% in $^{87}Sr/^{86}Sr$ and 1.2% in $^{87}Rb/^{86}Sr$. These errors were propagated through the age equation by a perturbation algorithm (Rees 1984).

The ^{40}Ar–^{39}Ar analysis followed the method described by Rex et al. (1993) with the following variations: Samples were irradiated at the Ford Reactor, Ann Arbor, Michigan, interference correction factors were (40/39)K = 0.03, (36/39)Ca = 1000 and (37/39)Ca = 0.24. An internal standard biotite (Rex and Guise 1986) was used in addition to interlaboratory hornblendes MMHb-1 and Hb3gr. Isotopic analyses were performed with a modified MS10 mass spectrometer, measured atmospheric $^{40}Ar/^{36}Ar$ was 288.8 $\pm$ 0.2% and sensitivity 1.35×10^{-7} cm3V-1.

Rb–Sr white mica ages

Eclogitic Micaschist Complex

Samples from the EMC yield ages from 30 Ma to 69 Ma (Table 1) and appear to show no systematic variation with geographical position or structural level (Fig. 4). Sample 56136 was collected very close to the 30 Ma Biella syenite intrusion, and may be discounted as reset during contact metamorphism. Otherwise, only 55498 shows evidence for significant retrogression, leaving a range of 52–69 Ma for samples that apparently comprise primary eclogite facies assemblages. Closely associated samples may show age differences of up to 14 Ma, suggesting that the ages are not simple cooling ages, since closely associated samples would have experienced the same thermal history. This is not surprising since the temperature estimates for the eclogite metamorphism are around 550 °C, the effective closure temperature for white mica Sr dating; the rocks did not experience a protracted high-temperature history that achieved thorough homogenisation. To explain the pattern of Rb–Sr ages in this unit, we must therefore appeal to factors other than purely thermally activated diffusion in white micas with a unique closure temperature and common thermal history.

Since there is no evidence of relict high-grade assemblages preserving Hercynian white micas, we can presume that the high-pressure assemblages crystallised with an entirely new white mica population. This is supported by reconnaissance SEM work that suggests that where compositional variation exists in EMC phengites, cores are of high-phengite (i.e. high-pressure) compositions. The oldest ages are therefore a minimum estimate for the age of the onset of high-pressure conditions. The range of ages obtained from the rest of the sample set suggests that Sr exchange continued to varying degrees after the peak of high-pressure

Table 1 Rb–Sr data for Eclogitic Micaschist Complex. (*EMS* eclogitic mica-schist)

Sample	Rb ppm Lithology	Sr ppm Location	$^{87}Sr/^{86}Sr$	$^{87}Rb/^{86}Sr$	Age $\pm$ 2SD
53960	EMS	Quinseina			
Phengite	283.4	58.6	0.72479	14.01	53.8 $\pm$ 0.7
Paragonite	71.7	378.6	0.71438	0.55	
Epidote	4.0	4111.4	0.71414	0.00	
54212	Marble	Pont Canavese			
Phengite	351.2	16.4	0.76403	62.42	63.3 $\pm$ 0.8
Calcite	0.4	432.9	0.70789	0.00	
54216	Marble	Quinseina			
Phengite	347.5	85.9	0.71695	11.71	57.0 $\pm$ 1.2
Calcite	4.7	1878.2	0.70748	0.01	
55217	Leucogneiss	Soglio			
Phengite 1	310.0	7.2	0.81224	126.52	52.3 $\pm$ 0.6
Phengite 2	307.0	6.4	0.82150	139.46	
Epidote	12.8	1763.7	0.71837	0.02	
55497	Leucogneiss	Quinseina			
Phengite	300.7	15.7	0.76680	55.81	59.8 $\pm$ 0.7
Epidote	15.1	6655.0	0.71940	0.01	
55498	EMS	Quinseina			
Phengite	297.5	495.7	0.72180	1.74	46.4 $\pm$ 2.1
Omphacite	8.2	346.3	0.72070	0.07	
55014	Marble	Chiaremonte, Val Chiusella			
Phengite	332.0	21.8	0.74732	44.20	63.0 $\pm$ 0.8
Calcite	1.0	315.6	0.70778	0.01	
55044	Marble	Quassolo			
Phengite	361.7	138.2	0.71553	7.58	64.5 $\pm$ 0.9
Calcite	0.0	887.6	0.70859	0.00	
55046	Marble	Fontainemore			
Phengite	299.6	3.2	0.94946	273.45	61.0 $\pm$ 0.7
Calcite	0.2	439.0	0.71086	0.00	
55045	Marble	Fontainemore			
Phengite	275.2	33.2	0.72999	23.05	58.5 $\pm$ 0.7
Calcite	0.3	571.2	0.71009	0.00	
Clinopyroxene	2.7	13.7	0.71046	0.57	
77519	EMS	Monte Mars			
Phengite	389.4	240.7	0.72414	4.71	68.8 $\pm$ 2.2
Clinopyroxene	87.6	116.2	0.72167	2.18	
56136	EMS	Monte Mucrone			
Phengite	353.8	340.8	0.71779	3.00	30.4 $\pm$ 1.3
Clinopyroxene	9.0	75.1	0.71664	0.35	
56128	EMS	Monte Mucrone			
Phengite	341.3	290.2	0.71714	3.41	53.8 $\pm$ 1.8
Clinopyroxene	15.0	36.2	0.71545	1.20	
56131	Metagranite	Monte Mucrone			
Phengite	356.4	51.8	0.73343	19.97	63.0 $\pm$ 1.3
Clinopyroxene/ Epidote	23.8	1409.2	0.71559	0.05	
56137	Eclogite	Monte Mucrone			
Phengite	178.1	198.5	0.70977	2.60	68.6 $\pm$ 3.1
Clinopyroxene	0.8	137.6	0.70726	0.02	

metamorphism. What processes might have controlled this exchange?

One possibility is that the temperatures during and immediately after the peak of metamorphism were close to the closure temperature for Sr, and that Sr exchange was achieved by volume diffusion in samples where local kinetic conditions were favourable. Minor deformation-induced recrystallisation would have favoured Sr exchange at these conditions (Inger and Cliff 1994), indeed the abundance of bent and kinked phengites in this unit suggests that unrecovered microstructural defects would be available to enhance Sr transport rates on a grain scale. Another option is that crystallisation of the peak assemblage occurred over

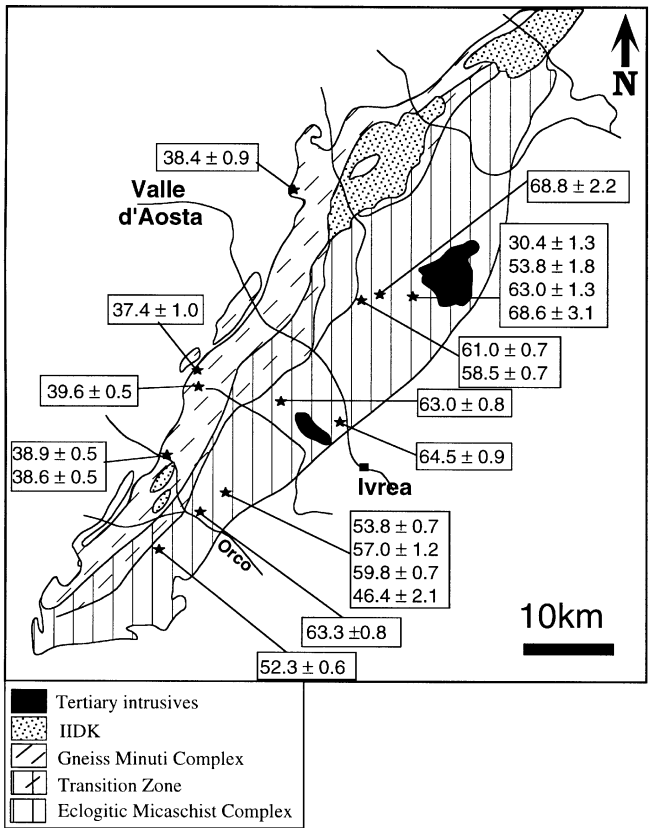

Fig. 4 Rb–Sr white mica ages from Sesia-Lanzo Zone (in Ma, 2-sigma errors)

a period of time, again controlled by local kinetics, yielding different near-crystallisation ages in different rocks.

Some samples may contain new retrograde mica growths, yielding a mixed age. The growth of partial overprinting assemblages may be assessed petrographically, although total recrystallisation of white mica may occur without replacement of the whole assemblage and might not be simple to distinguish. The micas analysed in this study all appear to be dominated by a single compositional generation, with in some cases a minor ($< 2\%$) overgrowth which would contribute very little to the Sr budget of the separate and hence would not shift the age significantly.

Age determinations may be sensitive to the choice of phases used to constrain initial $^{87}Sr/^{86}Sr$ ratios. The best minerals are those with low Rb/Sr ratios which should ideally have been open to Sr exchange with the micas during the event of interest. Carbonate is favoured because it dominates the Sr budget of calc-silicate rocks so would certainly have dominated the Sr reservoir with which micas were in equilibrium during growth, diffusive exchange, and possibly recrystallisation. Aragonite would be the stable carbonate phase at eclogite facies conditions. The inversion to calcite, although a form of retrogression, would not have disturbed the Sr distribution because the carbonate phase is by far the dominant Sr reservoir, and on the scale of our sampling would not have exchanged Sr with any other reservoir during inversion. It may however be prone to contamination by other Sr-rich carbonate phases introduced as veins by externally derived fluids. Omphacite is also used because it was probably growing as part of the high-pressure metamorphic assemblage at the same time as the phengites, and so incorporated the same bulk-rock Sr isotope ratio. If omphacite had a high T_c, and if the phengite (re)crystallised after omphacite growth it may not have exchanged Sr with the omphacite. The age yielded in this case would depend upon the phases with which the phengite *was* able to exchange Sr, and a phengite-omphacite age would fall between the growth and recrystallisation stages. Epidote has also been used to estimate initial $^{87}Sr/^{86}Sr$, but suffers from the suspicion that it may be a retrograde phase, or that it did not exchange Sr with micas because of a high T_c. Since the range of EMC ages do not show any systematic variation with the phase chosen to estimate initial ratio, we can say that some of the scatter in the age range may result from incomplete homogenisation between phengites and low-Rb/Sr phases, presumably *after* crystallisation of the peak metamorphic assemblage.

We conclude that the Rb–Sr ages from the EMC represent either:

1. Crystallisation and homogenisation of high-pressure assemblages over a period that spanned at least 70–55 Ma, or:
2. A partial resetting of pre-70 Ma Rb–Sr ages by an event younger than 55 Ma.

Gneiss Minuti Complex

Gneiss Minuti Complex samples present a much less ambiguous result, at least from the point of view of Rb–Sr dating (Table 2). Data clustering at 39.5 Ma strongly suggest either:

1. Regional cooling below blocking temperature at $\sim 39 \pm 1$ Ma, or:
2. Recrystallisation accompanied by thorough intercrystalline Sr equilibration at ~ 39 Ma.

An intriguing exception is sample 55017, which contains two mica compositions sufficiently different to be separated magnetically, and which yield different ages. This specimen is a highly strained calc-schist from the shear zone at the very base of the Sesia-Lanzo unit, where it overlies the Piémont unit. The strong fabric makes it impossible to distinguish the micas texturally. The easiest explanation would be that the 37.4 ± 1 Ma "white mica" crystallised during the greenschist facies shear event, whereas the more phengitic "green mica" is a relic of an earlier assemblage that was not fully recrystallised during the shear event. The 51.2 ± 0.6

Table 2 Rb–Sr data from Gneiss Minuti Complex (*WR* whole rock)

Sample	Rb ppm Lithology	Sr ppm Location	$^{87}Sr/^{86}Sr$	$^{87}Rb/^{86}Sr$	Age $\pm$ 2SD
54365	Schist	Bosco			
White mica	389.0	15.4	0.76270	73.45	38.9 $\pm$ 0.5
WR-mica	14.1	32.2	0.72283	1.27	
54369	Schist	Bosco			
White mica	396.6	14.8	0.76407	78.19	38.6 $\pm$ 0.5
WR-mica	17.3	20.9	0.72251	2.39	
55020	Calc-schist	Col de Bochetta, Val Chiusella			
White mica	423.3	54.8	0.72133	22.39	39.6 $\pm$ 0.5
Feldspar	2.2	46.5	0.70883	0.13	
Calcite	0.4	2098.9	0.70878	0.00	
55017	Calc-schist	Santanel, Val Soana			
White mica	496.2	41.1	0.72634	34.95	37.4 $\pm$ 1.0
Calcite	3.3	502.8	0.75393		
55017	Calc-schist	Santanel, Val Soana			
Green mica	566.6	25.9	0.75393	63.46	51.2 $\pm$ 0.6
Calcite	3.3	502.8	0.75393		
56140	Schist	Pallasina			
White mica	277.7	45.0	0.71995	17.87	38.4 $\pm$ 0.9
Epidote	11.9	1907.4	0.71020	0.02	

Ma age of the green mica may be close to its real age, since the carbonate Sr composition used as an initial ratio estimate is unlikely to have changed much and recrystallisation of the mineral would have resulted in a bulk composition at equilibrium with prevailing *P-T* conditions, i.e. the white mica.

We interpret the GMC Rb–Sr data as dating the pervasive development of a new fabric with very little remnant higher grade assemblage. The $\sim$ 39 Ma age has been found for a number of units showing this greenschist grade of fabric development (Hunziker et al. 1992; S Freeman, RWH Butler, S Inger, RA Cliff, submitted), and these results further confirm the generally accepted model that many units in the Western Alps suffered recrystallisation under greenschist-facies conditions at 39 Ma.

$^{40}Ar/^{39}Ar$ data

Eleven samples have been analysed for $^{40}Ar/^{39}Ar$ dating by step-release heating (Table 3). The release spectra are mostly well-defined plateaux (Fig. 5), which would usually be interpreted as representing undisturbed argon systematics. Plateau ages range from 39 Ma (in the GMC) to 93 Ma (in the EMC), with more disturbed spectra yielding steps in the 90–105 Ma range. The $^{40}Ar/^{39}Ar$ white mica ages are conventionally interpreted in terms of cooling through a closure temperature of $\sim$ 350 °C, but in these samples the $^{40}Ar/^{39}Ar$ are, with the exception of 55497, older than Sr ages from the same rocks. This shows that these data cannot be interpreted in terms of conventional cooling/T_c arguments unless extreme compositional effects (Scaillet et al. 1992) make the SLZ phengites so retentive for Ar that their T_c is substantially higher than 550 °C.

Excess argon, which would lead to spuriously old ages, can sometimes be identified from $^{39}Ar/^{40}Ar$ versus $^{36}Ar/^{40}Ar$ correlation plots. These can demonstrate a contribution of ^{40}Ar which is not accounted for by the air correction, and so does not result from radiogenic decay since the mineral was last closed to Ar loss. In most of our samples good correlations cannot be obtained because too many of the steps lie close to the $^{39}Ar/^{40}Ar$ axis (Fig. 5). Steps which fall on an apparently linear trend are those which account for the small proportion of gas released at low temperature. No excess radiogenic component was identified. The good plateaux show that the argon composition within these mineral grains is homogeneous with respect to retentivity in the furnace, which may or may not reflect retentivity during geological processes. The early, low-temperature steps may represent a contaminant in the less retentive – and therefore more easily reset – sites, or partial argon loss from those sites in a polymetamorphic history. Heterogeneous grain-scale argon compositions have been identified in sample 77519 (Kelley et al. 1993 and Reddy et al. *in press*), while Ruffet et al. (1995) showed widely variable ages but uniform grain-scale age maps and good plateau ages from closely spaced EMC rocks. Both studies concluded that conventional age determinations were being clouded by excess argon retained in the micas prior to cooling through closure temperature and introduced through microstructural defects. This problem has been widely identified in polymetamorphic and high-pressure rocks (Chopin and Maluski 1980), and may result from

Table 3 Step-release argon analyses

54212 White mica, run 1742, weight = 0.06051 g, J value = 0.005070 ± 0.5%
Integrated values, analytic and J errors (1 sigma)
Age (Ma) 68.57 0.15 0.69
*40/39 K 7.640 0.22%
Wt%K = 8.403, *40 = 228.23×10^{-7} cm^3g^{-1}

T °C	$^{39}Ar_K$ {----vol	$^{37}Ar_{Ca}$ $\times 10^{-9}$	$^{38}Ar_{Cl}$ cm^3---}	Ca/K	$*^{40}Ar/^{39}K$	%Atm	Age Ma	Error 1 sigma	$\%^{39}Ar$
670	2.755	2.086	0.038	1.507	6.786	63.1	61.03	2.18	1.5
770	10.492	1.116	0.123	0.212	7.354	23.0	66.04	0.40	5.8
830	88.877	0.301	1.057	0.007	7.736	8.3	69.41	0.11	49.2
875	21.513	0.000	0.258	0.000	7.911	6.5	67.43	0.19	11.9
960	26.433	0.017	0.314	0.001	7.525	5.7	67.55	0.23	14.6
1360	30.681	0.514	0.372	0.033	7.727	7.2	69.33	0.37	17.0

54216 White mica, run 1739, weight = 0.04518 g, J value = 0.004940 ± 0.5%
Integrated values, analytic and J errors(1 sigma)
Age (Ma) 69.78 0.28 0.74
*40/39 K 7.983 0.41%
Wt%K = 8.273, *40 = 228.73×10^{-7} cm^3g^{-1}

T °C	$^{39}Ar_K$ {----vol	$^{37}Ar_{Ca}$ $\times 10^{-9}$	$^{38}Ar_{Cl}$ cm^3---}	Ca/K	$*^{40}Ar/^{39}K$	%Atm	Age Ma	Error 1 sigma	$\%^{39}Ar$
650	1.321	0.607	0.039	0.914	7.661	47.7	67.02	6.31	1.0
750	5.033	0.915	0.057	0.362	7.767	42.5	67.93	1.53	3.9
800	36.715	0.193	0.443	0.010	8.078	18.6	70.59	0.39	28.4
845	41.231	0.000	0.487	0.000	7.971	6.3	69.67	0.35	31.8
900	10.533	0.060	0.124	0.011	7.966	7.5	69.63	0.63	8.1
1000	15.601	0.126	0.187	0.016	7.900	9.7	69.06	1.25	12.1
1340	19.021	0.321	0.232	0.034	7.982	7.6	69.77	0.68	14.7

55014 White mica, run 1862, weight = 0.04234 g, J value = 0.00650 ± 0.5%
Integrated values, analytic and J errors(1 sigma)
Age (Ma) 73.9 0.2 0.4
Wt%K = 6.6, *40 = 192×10^{-7} cm^3g^{-1}

T °C	$^{39}Ar_K$ {----vol	$^{37}Ar_{Ca}$ $\times 10^{-9}$	$^{38}Ar_{Cl}$ cm^3---}	Ca/K	$*^{40}Ar/^{39}K$	%Atm	Age Ma	Error 1 sigma	$\%^{39}Ar$
770	6.8	2.09	0.10	0.62	6.148	44.9	70.7	1.6	5.3
810	3.6	0.00	0.05	0.00	6.503	16.0	74.7	1.4	2.8
875	36.2	0.05	0.45	0.00	6.425	16.2	73.8	0.2	28.6
900	18.7	0.00	0.23	0.00	6.398	12.3	73.5	0.8	14.8
950	7.0	0.03	0.09	0.01	6.393	12.5	73.5	1.5	5.6
1005	8.3	0.00	0.10	0.00	6.351	13.3	73.0	0.7	6.6
1180	33.5	0.11	0.41	0.01	6.446	11.7	74.1	0.3	26.5
1325	12.4	0.00	0.15	0.00	6.679	11.4	76.7	1.0	9.8

55017 White mica, run 1863, weight = 0.03909 g, J value = 0.00650 ± 0.5%
Integrated values, analytic and J errors(1 sigma)
Age (Ma) 44.1 0.3 0.3
Wt%K = 7.6, *40 = 132×10^{-7} cm^3g^{-1}

T °C	$^{39}Ar_K$ {----vol	$^{37}Ar_{Ca}$ $\times 10^{-9}$	$^{38}Ar_{Cl}$ cm^3---}	Ca/K	$*^{40}Ar/^{39}K$	%Atm	Age Ma	Error 1 sigma	$\%^{39}Ar$
640	3.0	2.22	0.08	1.50	2.937	49.0	34.1	2.8	2.2
770	13.2	3.12	0.16	0.47	3.562	38.0	41.3	0.8	9.7
830	31.4	0.14	0.39	0.01	3.894	11.2	45.1	0.3	23.1
875	28.5	0.08	0.35	0.01	4.087	7.6	47.3	0.5	21.0
920	32.3	0.07	0.39	0.00	4.014	7.4	46.5	0.4	23.8
980	15.2	0.29	0.19	0.04	3.352	11.2	38.9	0.9	11.2
1110	10.1	0.00	0.12	0.00	3.405	7.0	39.5	0.9	7.4
1310	2.1	0.71	0.03	0.66	3.733	35.6	43.2	4.8	1.6

(*continued*)

Table 3 (continued)

55017 Green mica, run 1864, weight = 0.05793 g, J value = 0.00650 ± 0.5%
Integrated values, analytic and J errors(1 sigma)
Age (Ma) 39.5 0.2 0.2
Wt%K = 8.3, *40 = 128×10^{-7} cm^3g^{-1}

T °C	$^{39}Ar_K$ {----vol	$^{37}Ar_{Ca}$ $\times 10^{-9}$	$^{38}Ar_{Cl}$ cm^3---}	Ca/K	$^{*40}Ar/^{39}K$	%Atm	Age Ma	Error 1 sigma	$\%^{39}Ar$
660	4.4	4.21	0.11	1.89	3.094	65.0	35.9	2.8	2.0
765	9.2	1.40	0.11	0.30	3.348	9.4	38.8	1.0	4.2
840	35.4	0.02	0.43	0.00	3.337	12.6	38.7	0.2	16.2
900	101.2	0.18	1.23	0.00	3.412	5.7	39.6	0.1	46.4
950	43.6	0.03	0.53	0.00	3.431	4.0	39.8	0.4	20.0
1000	16.2	0.17	0.20	0.02	3.381	5.9	39.2	0.6	7.4
1120	7.1	0.34	0.08	0.10	3.753	8.1	43.5	1.2	3.3
1330	1.0	0.18	0.01	0.36	4.834	1.8	55.8	8.4	0.5

55020 White mica, run 1865, weight = 0.03823 g, J value = 0.00650 ± 0.5%
Integrated values, analytic and J errors(1 sigma)
Age (Ma) 59.8 0.3 0.4
Wt%K = 7.8, *40 = 185×10^{-7} cm^3g^{-1}

T °C	$^{39}Ar_K$ {----vol	$^{37}Ar_{Ca}$ $\times 10^{-9}$	$^{38}Ar_{Cl}$ cm^3---}	Ca/K	$^{*40}Ar/^{39}K$	%Atm	Age Ma	Error 1 sigma	$\%^{39}Ar$
650	1.2	3.51	0.03	6.00	4.716	66.4	54.5	7.3	0.9
755	4.1	3.19	0.06	1.54	4.461	54.0	51.6	3.3	3.0
800	14.5	0.23	0.18	0.03	4.945	16.3	57.1	0.7	10.7
855	50.1	0.18	0.62	0.01	5.368	7.2	61.9	0.2	36.7
900	31.8	0.02	0.39	0.00	5.232	8.0	60.3	0.4	23.3
945	18.5	0.02	0.23	0.00	4.887	7.0	56.4	0.8	13.6
1000	8.0	0.04	0.10	0.01	4.797	13.3	55.4	0.7	5.8
1100	5.8	0.00	0.07	0.00	5.589	2.8	64.4	2.1	4.2
1320	2.5	0.09	0.03	0.07	6.308	0.1	72.5	5.0	1.9

55044 White mica, run 1868, weight = 0.04377 g, J value = 0.00650 ± 0.5%
Integrated values, analytic and J errors(1 sigma)
Age (Ma) 70.9 0.2 0.4
Wt%K = 7.9, *40 = 222×10^{-7} cm^3g^{-1}

T °C	$^{39}Ar_K$ {----vol	$^{37}Ar_{Ca}$ $\times 10^{-9}$	$^{38}Ar_{Cl}$ cm^3---}	Ca/K	$^{*40}Ar/^{39}K$	%Atm	Age Ma	Error 1 sigma	$\%^{39}Ar$
665	5.0	6.95	0.13	2.78	5.856	64.9	67.4	1.3	3.2
755	7.9	5.63	0.09	1.42	6.254	28.1	71.9	0.9	5.0
820	15.3	0.65	0.19	0.09	6.288	28.3	72.3	1.1	9.7
860	41.8	0.49	0.51	0.02	6.159	22.9	70.8	0.3	26.5
900	20.5	0.12	0.26	0.01	6.110	22.1	70.3	0.6	13.0
955	19.3	0.09	0.24	0.01	6.136	24.9	70.6	0.7	12.3
1005	25.7	0.06	0.31	0.01	6.217	21.2	71.5	0.3	16.3
1120	12.9	0.06	0.16	0.01	6.052	22.0	69.6	0.5	8.2
1380	9.1	0.28	0.12	0.06	6.330	44.6	72.8	1.3	5.8

Table 3 (continued)

55045 White mica, run 1866, weight = 0.05613 g, J value = 0.006500 ± 0.5%
Integrated values, analytic and J errors(1 sigma)
Age (Ma) 95.70 0.20 0.51
*40/39 K 8.382 0.22%
Wt%K = 7.701, *40 = 294.16×10^{-7} cm^3g^{-1}

T °C	$^{39}Ar_K$ {----vol	$^{37}Ar_{Ca}$ $\times 10^{-9}$	$^{38}Ar_{Cl}$ cm^3---}	Ca/K	$*^{40}Ar/^{39}K$	%Atm	Age Ma	Error 1 sigma	$\%^{39}Ar$
660	1.232	7.765	0.268	12.544	8.261	75.5	94.36	9.56	0.6
750	3.852	25.133	0.081	12.985	9.067	28.9	103.32	1.25	2.0
805	5.807	0.588	0.096	0.202	9.229	17.2	105.10	1.50	2.9
860	55.841	0.149	0.745	0.005	7.875	8.4	90.07	0.20	28.3
905	44.283	0.104	0.594	0.005	8.152	6.2	93.15	0.29	22.5
960	31.237	0.109	0.420	0.007	8.388	7.4	95.77	0.38	15.9
1006	16.710	0.575	0.245	0.068	9.291	8.5	105.79	0.51	8.5
1120	13.814	2.688	0.193	0.387	9.237	7.0	105.20	0.54	7.0
1340	24.219	2.902	0.321	0.238	8.538	4.2	97.44	0.28	12.3

55046 White mica, run 1867, weight = 0.03066 g, J value = 0.006500 ± 0.5%
Integrated values, analytic and J errors(1 sigma)
Age (Ma) 90.89 0.31 0.54
*40/39 K 7.950 0.35%
Wt%K = 9.109, *40 = 330.00×10^{-7} cm^3g^{-1}

T °C	$^{39}Ar_K$ {----vol	$^{37}Ar_{Ca}$ $\times 10^{-9}$	$^{38}Ar_{Cl}$ cm^3---}	Ca/K	$*^{40}Ar/^{39}K$	%Atm	Age Ma	Error 1 sigma	$\%^{39}Ar$
660	1.301	0.602	0.020	0.920	7.504	72.9	85.91	11.85	1.0
755	4.747	0.913	0.063	0.383	7.891	33.8	90.24	1.83	3.7
790	5.474	0.013	0.071	0.005	8.026	19.0	91.75	2.48	4.3
855	47.638	0.031	0.603	0.001	7.959	18.7	91.00	0.12	37.4
900	32.242	0.020	0.415	0.001	7.916	14.1	90.52	0.50	25.3
965	19.485	0.038	0.253	0.004	7.838	13.4	89.64	0.72	15.3
990	5.290	0.036	0.066	0.014	7.759	17.7	88.77	1.37	4.2
1120	6.854	0.044	0.086	0.013	8.118	9.1	92.77	1.02	5.4
1320	4.243	0.256	0.059	0.120	8.682	9.6	99.04	2.99	3.3

55497 White mica, run 1740, weight = 0.05245 g, J value = 0.00494 ± 0.5%
Integrated values, analytic and J errors(1 sigma)
Age (Ma) 51.92 0.16 0.54
*40/39 K 5.910 ± 0.31%
Wt%K = 10.170, *40 = 208.17×10^{-7} cm^3g^{-1}

T °C	$^{39}Ar_K$ {----vol	$^{37}Ar_{Ca}$ $\times 10^{-9}$	$^{38}Ar_{Cl}$ cm^3---}	Ca/K	$*^{40}Ar/^{39}K$	%Atm	Age Ma	Error 1 sigma	$\%^{39}Ar$
665	4.213	0.091	0.114	0.043	4.245	55.0	37.44	1.68	2.3
740	6.457	0.079	0.074	0.024	5.485	20.5	48.23	0.60	3.5
800	12.550	0.000	0.154	0.000	5.639	7.2	49.57	0.56	6.8
830	13.417	0.000	0.157	0.000	5.705	6.1	50.14	0.35	7.3
900	45.763	0.000	0.539	0.000	6.014	4.2	52.82	0.44	24.8
995	62.669	0.000	0.738	0.000	5.3917	3.8	51.97	0.17	33.9
1170	37.281	0.118	0.434	0.006	6.152	4.1	54.01	0.14	20.2
1320	2.401	0.226	0.031	0.187	6.604	15.0	57.92	1.85	1.3

(*continued*)

Table 3 (continued)

77519 White mica (a), run 2132, weight = 0.03393 g, J value = 0.003900 ± 0.5%
Integrated values, analytic and J errors(1 sigma)
Age (Ma) 95.54 0.31 0.56 (93.9 ± 0.56 Ma without final step – probably contaminated)
*40/39 K 13.945 ± 0.33%
Wt%K = 8.908, *40 = 339.67×10^{-7} cm^3g^{-1}

T °C	$^{39}Ar_K$ {----vol	$^{37}Ar_{Ca}$ $\times 10^{-9}$	$^{38}Ar_{Cl}$ cm^3---}	Ca/K	$^{*40}Ar/^{39}K$	%Atm	Age Ma	Error 1 sigma	$\%^{39}Ar$
626	1.336	0.034	0.062	0.051	13.532	44.2	92.79	1.68	1.6
742	4.214	0.000	0.059	0.000	14.137	23.7	96.82	1.31	5.1
802	7.124	0.036	0.093	0.010	13.834	21.2	94.80	1.12	8.6
849	22.881	0.008	0.296	0.001	13.531	13.7	92.77	0.86	27.7
908	18.844	0.000	0.248	0.000	13.832	13.2	94.79	0.20	22.8
946	12.581	0.009	0.164	0.001	13.688	14.0	93.83	0.12	15.2
1001	7.410	0.000	0.097	0.000	13.587	14.6	93.15	0.30	9.0
1095	4.354	0.007	0.059	0.003	13.609	11.8	93.30	0.61	5.3
1325	3.902	0.242	0.107	0.123	18.936	5.6	128.54	0.54	4.7

77519 White mica (b), run 2133, weight = 0.03063 g, J value = 0.003900 ± 0.5%
Integrated values, analytic & J errors(1 sigma)
Age (Ma) 94.14 0.13 0.58
*40/39 K 13.735 ± 0.15%
Wt%K = 8.996 ,*40 = 337.87×10^{-7} cm^3g^{-1}

T °C	$^{39}Ar_K$ {----vol	$^{37}Ar_{Ca}$ $\times 10^{-9}$	$^{38}Ar_{Cl}$ cm^3---}	Ca/K	$^{*40}Ar/^{39}K$	%Atm	Age Ma	Error 1 sigma	$\%^{39}Ar$
662	2.613	0.036	0.073	0.027	14.116	39.2	96.68	1.00	3.5
748	5.953	0.000	0.082	0.000	13.999	17.4	95.90	0.39	7.9
808	22.171	0.104	0.287	0.009	13.610	16.2	93.31	0.12	29.4
850	17.608	0.000	0.228	0.000	13.849	12.2	94.90	0.22	23.4
904	11.218	0.048	0.143	0.009	13.786	14.5	94.48	0.26	14.9
950	7.789	0.000	0.099	0.000	13.496	11.3	92.55	0.27	10.3
1000	3.481	0.028	0.044	0.016	13.463	10.2	92.32	0.69	4.6
1100	2.460	0.000	0.029	0.000	13.894	7.9	95.20	1.29	3.3
1320	2.056	0.178	0.031	0.173	13.739	15.9	94.17	1.69	2.7

inwards migration of Ar from a fluid phase, or the absence of a suitable fluid phase to enhance grain boundary diffusive venting of argon during the high-pressure metamorphic stage.

Like Ruffet et al. (1995) and Arnaud and Kelley (1995), we interpret our $^{40}Ar/^{39}Ar$ data as indicating a mixed Ar composition within the grains that was produced by an externally derived excess radiogenic component and an in situ radiogenic component that grew by K-decay within the crystal. The two (or more) components may originally have resided in different crystallographic sites, perhaps related to deformation-accommodating crystal defects, but they are thoroughly mixed on the scale of the domains accessed by the step-heating technique. The fact that flat plateaux are yielded by micas from 77519, whereas Reddy et al. (*in press*) show a rim to core gradient from older to younger ages on a microscopic scale, certainly demonstrates that release spectra do not reveal internal heterogeneities in Ar compostion, and are therefore geochronologically meaningless in this case. It must surely call into question the widespread reliance upon $^{40}Ar/^{39}Ar$ and K–Ar dates to constrain the age of the high-pressure metamorphism in the Sesia-Lanzo Zone.

U–Pb data

Sphenes from five calc-silicate samples (four EMC, one GMC) were analysed by the U–Pb dating technique, taking the initial Pb composition to be that of a co-existing low-μ phase such as white mica or feldspar (Table 4). Given the low U content of these rocks, it is unlikely that the bulk-rock Pb isotope composition changed significantly over the time span of the Alpine events, so this measurement is a reliable estimate of the Pb incorporated into sphene when it crystallised.

Of the four samples from the EMC, 54216 gives a good concordant age at 66 Ma, while 55044 gives an indistinguishable age albeit with a larger error in $^{207}Pb^*/^{235}U$ (Fig. 6). The other EMC samples give

a concordant age at 141 ± 1 Ma and a discordant result with a $^{206}Pb/^{238}U$ age of 107 ± 1.5 Ma.

Interpretation of the sphene ages relies on understanding their crystallisation age in relation to the metamorphic assemblage. Sphenes 54216 and 55044 both come from rocks which show only one metamorphic assemblage, that of the high-pressure event, and can be assigned to the monometamorphic sequence on the maps of Venturini et al. (1991, 1994). It is therefore likely that these minerals crystallised during the high-pressure metamorphism and retain Pb from only that event. The other samples are from rocks with a clear polymetamorphic history – they contain relic augitic pyroxenes as well as omphacite – and the Pb inheritance is likely since the high-pressure recrystallisation was at a temperature too low for the complete re-opening of sphene to Pb diffusion. The 66 ± 1 Ma ages probably record crystallisation during the high-pressure metamorphism. The 141 Ma ages probably reflect mixtures of old (Hercynian?) and Alpine sphene generations with different Pb signatures. Although 55045 appears concordant, it is equally compatible with a Hercynian age (~ 300–250 Ma) sphene population that underwent overgrowth or partial Pb loss at around 65 Ma.

The radical discordance of 55046 is difficult to explain by Pb loss after a Hercynian event, since it lies on a discordia with an upper intercept at 1.5 Ga, and it is extremely unlikely that relic sphene would survive for that length of time. It may have been caused by contamination by detrital zircon in this sample.

The GMC sphene (55020) yields a nearly concordant age of ~ 249 Ma. Its composition can be modelled by

Fig. 5 $^{40}Ar - {}^{39}Ar$ step-release spectra and correlation plots for samples from the Eclogitic Micaschist Complex (**a**) and Gneiss Minuti Complex (**b**). Regressions plotted by Isoplot (Ludwig 1990). No meaningful regression could be plotted for 55497 because data are too clustered

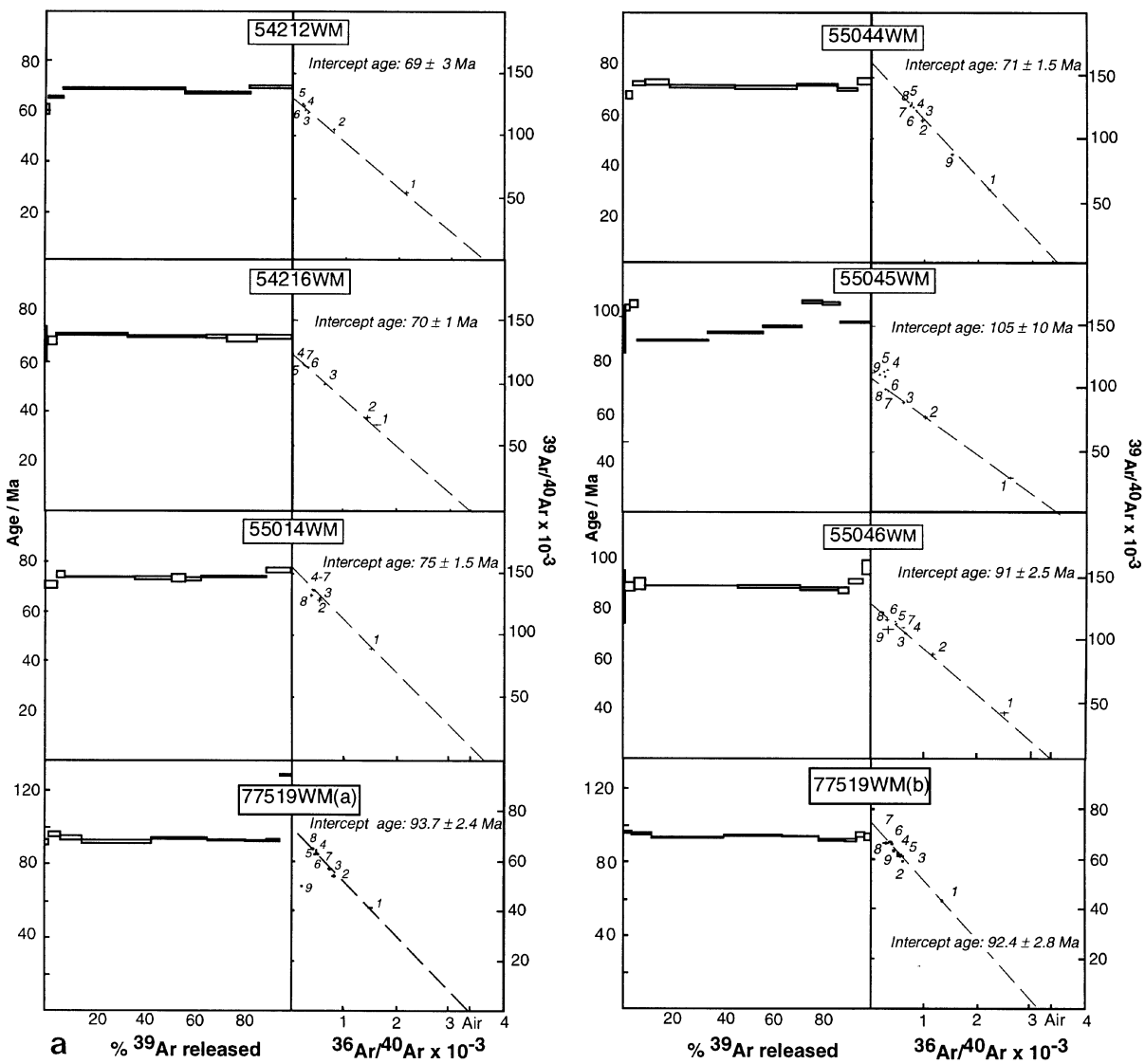

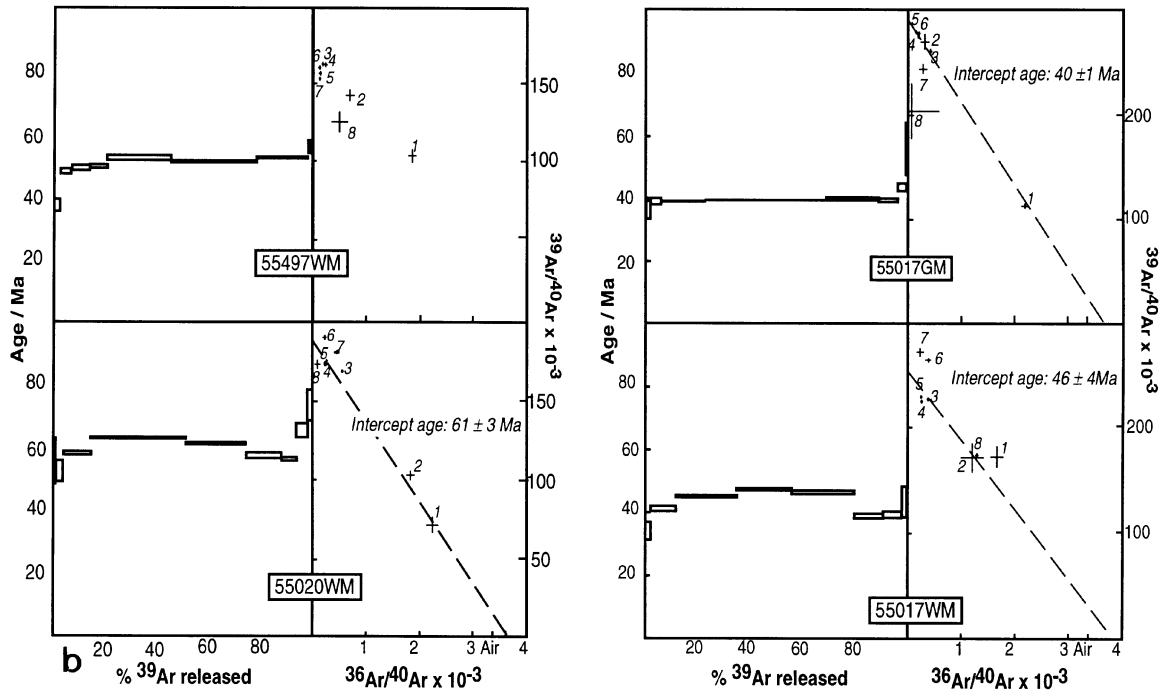

Fig. 5 (continued)

10% lead loss (or overgrowth) at 65–40 Ma on a population originally crystallised at ~ 280 Ma, its probable Hercynian age. Rejuvenation of the sphene population was clearly limited in the pervasive greenschist event, and this rock clearly did not crystallise abundant new sphene-bearing assemblages during any presumed high-pressure period of its history.

Interpreting the age data

Data from the three isotope systems have been plotted on conventional temperature-time plots, taking the closure temperatures from Cliff (1993). These re-emphasise the problem of interpreting the $^{40}Ar/^{39}Ar$ ages by closure temperature. They do however show concordance between the systems in the monometamorphic lithologies. It is interesting to note that notwithstanding their anomalously old ages, the Ar data from the monometamorphic samples form the least disturbed spectra. In the light of these isotopic studies, the metamorphic history of the Sesia-Lanzo Zone can be described as follows;

Hercynian orogenic events are preserved in some sphene populations from polymetamorphic basement rocks; Pb isotopes yield mixed ages reflecting partial resetting or new sphene growth during the Alpine cycle in the Eclogitic Micaschist Complex. Monometamorphic assemblages yield sphene U–Pb ages of 66 ± 1 Ma, recording sphene growth close to the high-pressure metamorphic climax. The Rb–Sr white mica ages in these samples are younger than the sphene ages, reflecting either cooling below phengite closure, or re juvenation of the Rb–Sr system during recrystallisation.

The Rb–Sr data from the EMC suggest a period of at least 16 Ma over which high-pressure phengites were stable. This is consistent with the macrostructural and textural evidence that under eclogite facies conditions, the EMC underwent a fabric-forming metamorphism/deformation event and subsequent non-penetrative deformation which locally recrystallised the planar fabric (T_E) into folds and crenulation cleavages (T_{cc}). Such local effects have at least partially reset the Sr systems in rocks, giving a spread of ages which constrains the timing of recrystallisation under those *P-T* conditions to be no older than 70 Ma, possibly younger than 54 Ma.

The $^{40}Ar/^{39}Ar$ data are difficult to interpret because of the widespread presence of excess argon in both polymetamorphic and monometamorphic units at all grades. Argon may be controlled by factors other than thermal diffusion rates, and it seems likely that grain boundary fluid compositions and connectivity did not allow resetting of the ^{40}Ar–^{39}Ar system during eclogite or greenschist facies metamorphism in these samples. (Resetting of this system requires removal of Ar from the rock, contrasting with the Rb-Sr system which is reset by exchange of Sr across grain boundaries, and does not require a carrier fluid.)

Table 4 U–Pb mineral data from the Sesia-Lanzo Zone. Initial ratios from phengite except [f] from feldspar

Sample Mineral	54216 Sphene	55020 Sphene	55044 Sphene	55045 Sphene	55046 Sphene
Pb ppm	3.27 ± 0.07	12.02 ± 0.24	8.97 ± 0.20	9.62 ± 0.31	8.68 ± 0.22
U ppm	124.9 ± 0.8	226.08 ± 1.35	33.74 ± 0.05	85.31 ± 0.32	204.04 ± 1.36
$^{206}Pb/^{204}Pb$	58.87 ± 0.21	357.85 ± 1.48	21.33 ± 0.009	39.73 ± 0.06	74.49 ± 0.14
$^{207}Pb/^{204}Pb$	17.63 ± 0.07	33.13 ± 0.12	15.80 ± 0.008	16.77 ± 0.02	18.56 ± 0.026
$^{208}Pb/^{204}Pb$	39.43 ± 0.19	129.63 ± 0.54	39.36 ± 0.02	49.48 ± 0.08	67.43 ± 0.10
$^{206}Pb/^{204}Pb_{initial}$	18.98 ± 0.05	20.00 ± 0.06[f]	18.70 ± 0.02	21.10 ± 0.02	18.36 ± 0.04
$^{207}Pb/^{204}Pb_{initial}$	15.78 ± 0.05	15.71 ± 0.04[f]	15.69 ± 0.02	15.86 ± 0.01	14.76 ± 0.04
$^{208}Pb/^{204}Pb_{initial}$	39.01 ± 0.15	39.61 ± 0.14[f]	38.78 ± 0.04	40.22 ± 0.04	36.58 ± 0.12
$^{206}Pb^*/^{238}U$	0.01034 ± 0.00006	0.039 ± 0.0003	0.0102 ± 0.0001	0.0221 ± 0.0001	0.0168 ± 0.0001
$^{207}Pb^*/^{235}U$	0.0664 ± 0.0031	0.278 ± 0.002	0.0585 ± 0.010	0.150 ± 0.004	0.157 ± 0.003
Age ($^{206}Pb/^{238}U$) Ma	66.3 ± 0.4	250 ± 2	65.5 ± 0.6	141.0 ± 0.7	107.0 ± 1.5
Age ($^{207}Pb/^{235}U$) Ma	65.3 ± 3.0	248 ± 2	58 ± 10	142 ± 4	147 ± 3

The pervasive fabric-forming greenschist facies event in the GMC is well constrained at 39 ± 1 Ma from Rb–Sr data. Previous studies (Hunziker et al. 1993) have interpreted K–Ar and Ar–Ar ages from this unit as recording cooling below 350 °C. If they are indeed cooling ages, the concordance with Rb–Sr indicates a fast period of cooling after fabric formation. We prefer to interpret them as close to recrystallisation ages at low temperatures.

Metamorphic conditions at the time were inappropriate for new sphene growth in certain lithologies, and temperatures were too low to rejuvenate sphene U–Pb systems significantly. It is unclear whether the fabric-forming event corresponds to the greenschist thermal peak. The recognition of an older, higher pressure mica generation (55017 "green mica") in the shear zone that juxtaposes GMC and Piémont units suggests that an earlier higher pressure assemblage was overprinted by a fabric related to that shearing event at 39 Ma. The early mica generation yields a $^{40}Ar/^{39}Ar$ age slightly older than the later micas Rb–Sr age. The early micas were probably reset during the greenschist event and cooled below their blocking temperature before the later generation of micas were generated in a low-temperature shear event. These later micas incorporated volatile components from a mixed and changing source, including an externally derived Ar component that resulted in their spurious ages. This explanation is supported by the field observation that the rock comes from the lowermost levels of the Gneiss Minuti where a chaotic and partly brittle shear zone emplaces it against the Piémont unit.

Geological implications

Two models have been proposed for the mechanical contiguity of the Sesia-Lanzo Zone during the Alpine orogeny:

1. It represents three or more tectonic slices that were juxtaposed during the Alpine collision, and therefore record individual tectonic and metamorphic histories prior to this assembly .
2. The GMC and EMC represent a single unit of crust that was subjected to early-Alpine high-pressure metamorphism throughout. During uplift and exhumation, the locus of deformation and metamorphism migrated westwards into the lower levels, so that the GMC records lower grade metamorphism and strain which did not occur in the EMC.

Although the new isotopic data do not unequivocally distinguish between the two models, they suggest that the EMC recrystallisation resulted in new sphene growth that did not occur in similar lithologies in the GMC. Either the GMC never experienced eclogite facies conditions, or high-pressure assemblages were sporadically developed as a consequence of local kinetic effects. The former explanation accords with the structural-metamorphic studies of Passchier et al. (1981) and Williams and Compagnoni (1983), that demonstrated a difference in metamorphic history across the EMC-GMC contact. Juxtaposition of EMC and GMC in the middle crust had occurred before 38 Ma, by which time penetrative deformation had migrated down-section to the west and generated greenschist facies fabrics throughout the GMC and locally in the transition zone. Ductile deformation in this unit effectively terminated by ~ 37 Ma.

The emplacement of the IIDK above, and in some cases between, the EMC and GMC remains problematic because the IIDK did not experience temperatures higher than 350 °C during the Alpine cycle. The contact has been re-oriented by later deformation, and is variably defined by blueschist and greenschist strain fabrics, suggesting that it was active later than 37 Ma, as temperatures at these crustal levels waned during uplift. The 30 Ma pyroclastic flows along the Canavese Line contain clasts of eclogitic EMC and have been

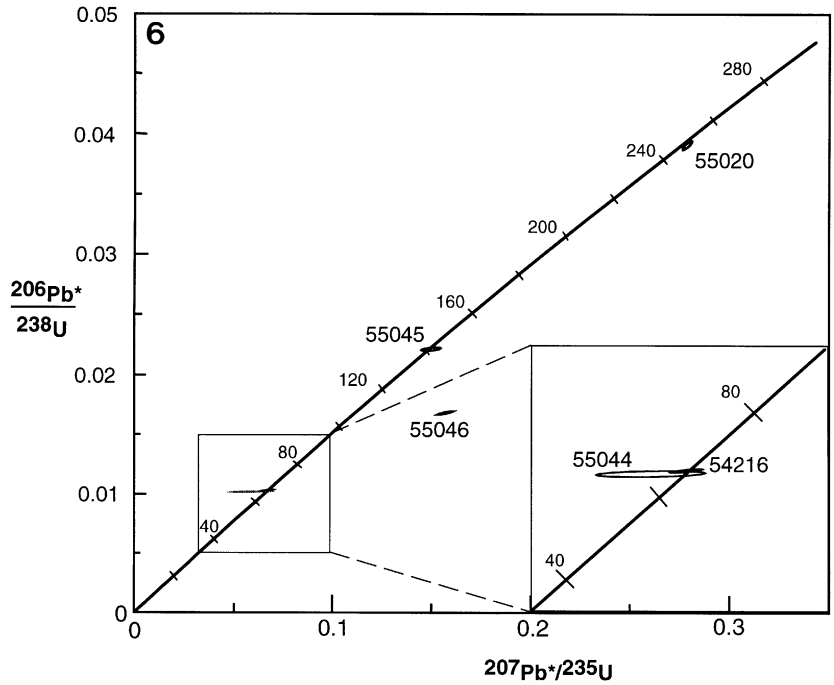

Fig. 6 U–Pb concordia diagram for samples from the Eclogitic Micaschist Complex and Gneiss Minuti Complex

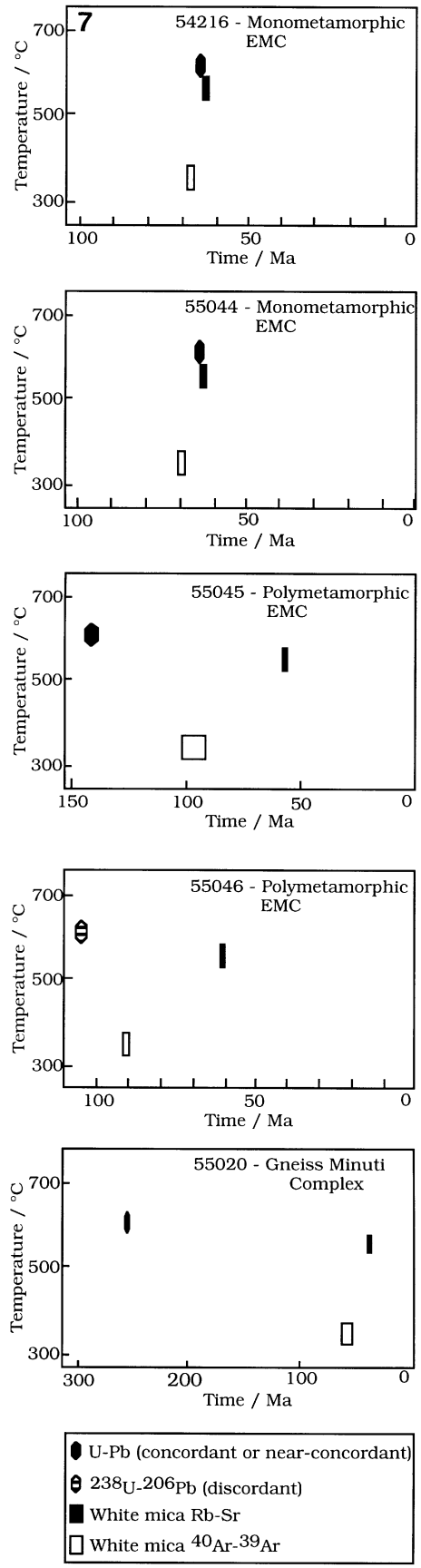

Fig. 7 Conventional "temperature-time" plots for five samples based on U–Pb (sphene), ^{40}Ar–^{39}Ar and Rb–Sr closure temperatures given in Cliffs (1993)

interpreted as the Oligocene cover to the Sesia-Lanzo Zone (Scheuring et al. 1974). This implies that the EMC was exposed at the surface at that time, and constrains the EMC-IIDK juxtaposition to pre-30 Ma. An average exhumation rate can be estimated for the EMC of 1.5 mm/year since high-pressure metamorphism, and 3–4 mm/year after the greenschist event in the GMC.

On a broader scale, the data indicate that high-pressure metamorphic fabrics in the Eclogitic Micaschist Complex of the SLZ formed and deformed in the 70–60 Ma period. The best estimate for the metamorphic peak is given by sphene U–Pb ages at 66 Ma. This contrasts with previous work that suggested a metamorphic peak at 100–140 Ma and cooling through phengite argon closure at 350 °C at 70 Ma. The Sesia-Lanzo Zone is so-called Austroalpine crust of African affinity, and it has always been problematic to explain why the unit was at eclogite facies from the early to the middle Cretaceous. The only way to maintain such a low geothermal gradient in continental crust is to establish a subduction zone adjacent to thickened continental crust, or to subduct the crust itself to depths of over 40 km (Ernst 1975). In the early Cretaceous, however, the Austroalpine was a passive margin bounding the actively-extending Tethyan basin

(Coward and Dietrich 1989), a setting difficult to reconcile with a thickened crust and subduction zone.

The new data suggest that the onset of convergent processes in the middle Cretaceous and the establishment of an accretionary wedge resulted in subduction of a crustal sliver, including Middle Jurassic platform sediments (Venturini et al. 1994), to depths of > 30 km by 70 Ma. These were then returned to mid-crustal levels in < 30 million years. Moreover, this model is consistent with data from the Austroalpine domain of the central and eastern Alps, where eclogite facies was not attained, but the onset of subduction is stratigraphically constrained to be late-Cretaceous (Frisch et al. 1987). There is no need to invoke a long-lived subduction zone to maintain a depressed geothermal gradient for 70 million years in the Western Alps.

Acknowledgements This work was funded by a NERC Research Grant (GR3/7820) to R.A.C. and a NERC Research Studentship (W.R.). We are grateful to Prof Roberto Compagnoni for an expert introduction to the rocks of the Sesia-Lanzo region. Thanks to Tom Oddy, Rod Green and Phil Guise for technical assistance, and to Simon Kelley and Giles Droop for pertinent reviews.

References

Arnaud NO, Kelley SP (1995) Evidence for excess argon during high pressure metamorphism in the Dora Maira Massif (western Alps, Italy), using an ultra-violet laser ablation microprobe ^{40}Ar–^{39}Ar technique. Contrib Mineral Petrol 121:1–11

Becker H (1993) Garnet peridotite and eclogite Sm-Nd mineral ages from the Lepontine dome (Swiss Alps): new evidence for Eocene high-pressure metamorphism in the central Alps. Geology 21:599–602

Bowtell SA, Cliff RA, Barnicoat AC (1994) Sm–Nd isotopic evidence on the age of eclogitization in the Zermatt-Saas ophiolite. J Metamorphic Geol 12:187–196

Chopin C, Maluski H (1980) ^{40}Ar–^{39}Ar dating of high-pressure metamorphic micas from the Gran Paradiso area (Western Alps): evidence against the blocking temperature concept. Contrib Mineral Petrol 74:109–122

Cliff RA (1993) Isotopic dating of metamorphism and cooling. In: Proc VI Summer School Earth Planet Sci, Siena, pp 131–140

Compagnoni R (1977) The Sesia-Lanzo Zone: high pressure-low temperature metamorphism in the Austroalpine continental margin. Rend Soc Ital Mineral Petrol 33:335–375

Compagnoni R, Dal Piaz GV, Hunziker JC, Gosso G, Lombardo B, Williams PF (1977) The Sesia-Lanzo Zone, a slice of continental crust with Alpine high pressure-low temperature assemblages in the Western Alps. Rend Soc Ital Mineral Petrol 33:281–334

Coward M, Dietrich D (1989) Alpine tectonics – an overview. In: Coward MP, Dietrich D, Park RG (eds) Alpine tectonics. Geol Soc Spec Publ 45:1–29

Ernst WG (1975) Systematics of large-scale tectonics and age progression in Alpine and circum-Pacific blueschist belts. Tectonophysics 26:229–246

Frisch W, Gommeringer K, Kelm U, Popp F (1987) The Upper Bündner Schiefer of the Tauern Window – a key to understanding Eoalpine orogenic processes in the Eastern Alps. In: Flügel HW, Faupl P (eds) Geodynamics of the Eastern Alps. Franz Deuticke, Vienna, pp 55–69

Hunziker JC, Desmons J, Hurford AJ (1992) Thirty-two years of geochronological work in the Central and Western Alps: a review on seven maps. Mem Geol Lausanne 13

Hunziker JC, Desmons J, Martinotti G (1989) Alpine thermal evolution in the central and the western Alps. In: Coward MP, Dietrich D, Park RG (eds) Alpine tectonics. Geol Soc Spec Publ 45:353–367

Inger S, Cliff RA (1994) Timing of metamorphism in the Tauern Window, Eastern Alps: Rb–Sr ages and fabric formation. J Metamorphic Geol 12:695–707

Kelley SP, Reddy SM, Wheeler J, Butler RH, Knipe RJ (1993) High spatial resolution laser $^{40}Ar/^{39}Ar$ dating on deformed micas from the Sesia Zone. Terra Abstr 5:388–389

Kwan TS, Krähenbuhl R, Jäger E (1992) Rb-Sr, K-Ar and fission track ages for granites from Penang Island, West Malaysia: an interpretation model for Rb-Sr whole rock and for actual and experimental mica data. Contrib Mineral Petrol 111:527–542

Lardeaux JM, Spalla MI (1991) From granulites to eclogites in the Sesia Zone (Italian Western Alps): a record of the opening and closure of the Piedmont ocean. J Metamorphic Geol 9:35–59

Ludwig KR (1990) Isoplot: a plotting and regression program for radiogenic-isotope data, for IBM-PC compatible computers, version 2.03. U S Geol Surv Open-File Rep 88–557

Marquer D, Peucat JJ (1994) Rb-Sr systematics of recrystallised shear zones at the greenschist-amphibolite transition – examples from granites in the Swiss Central Alps. Schweiz Mineral Petrogr Mitt 74:343–358

Mezger K, Rawnsley SR, Bohlen SR, Hanson GN (1991) U-Pb garnet, titanite, monazite and rutile ages: implications for the duration of high grade metamorphism and cooling histories. J Geol 99:415–428

Oberhänsli R, Hunziker JC, Martinotti G, Stern WB (1985) Geochemistry, geochronology and petrology of Monte Mucrone: an example of Eo-Alpine eclogitisation of Permian granitoids in the Sesia-Lanzo Zone, Western Alps, Italy. Chem Geol Isot Geosci Sect 52:165–184

Passchier CW, Urai JL, Van Loon J, Williams PF (1981) Structural geology of the central Sesia-Lanzo Zone. Geol Mijn 60: 497–507

Pognante U (1989) Lawsonite, blueschist and eclogite formation in the southern Sesia Zone (western Alps, Italy). Eur J Mineral 1:89–104

Pognante U, Talarico F, Rastelli N, Ferrati N (1987) High pressure metamorphism in the nappes of the Valle dell'Orco traverse (Western Alps collisional belt). J Metamorphic Geol 5:397–414

Ramsbotham W, Inger S, Cliff RA, Rex D, Barnicoat A (1994) Time constraints on the metamorphic and structural evolution of the southern Sesia-Lanzo Zone, Western Italian Alps. Mineral Mag 58A:758–759

Reddy SM, Kelley SP, Wheeler J (1996) A ^{40}Ar–^{39}Ar laser probe study of micas from the Sesia Zone, Italian Alps: implications for metamorphic and deformation histories. J Metamorphic Geol (in press)

Rees CE (1984) Error propagation calculations. Geochim Cosmochim Acta 48:2309–2311

Rex DC, Guise PG (1986) Age of the Tinto Felsite, Lanarkshire: a possible 39Ar–40Ar monitor. Bull Liaison Information, I.G.C.P. Project 196, No 6

Rex DC, Guise PC, Wartho J-A (1993) Disturbed ^{40}Ar-^{39}Ar spectra from hornblendes: thermal loss or contamination? Chem Geol Isot Geosci Sect 103:271–281

Ridley J (1989) Structural and metamorphic history of a segment of the Sesia-Lanzo Zone, and its bearing on the kinematics of Alpine deformation in the western Alps. In: Coward MP, Dietrich D, Park, RG (eds) Alpine tectonics. Geol Soc Spec Publ 45:pp189–201

Rubie DC (1984) A thermal-tectonic model for high-pressure metamorphism and deformation in the Sesia Zone, Western Alps. J Geol 92:21–36

Ruffet G, Féraud G, Ballèvre M, Kienast J-R (1995) Plateau ages and excess argon in phengites: an ^{40}Ar–^{39}Ar laser probe study of Alpine micas (Sesia Zone, Western Alps, northern Italy). Chem Geol Isot Geosci Sect 121:327–343

Scaillet S, Feraud G, Ballèvre M, Amouric M (1992) Mg/Fe and [(Mg,Fe)Si-Al_2] compositional control on argon behaviour in white micas: a $^{40}Ar/^{39}Ar$ continuous laser-probe study from the Dora-Maira nappe of the internal western Alps, Italy. Geochim Cosmochim Acta 56:2851–2872

Scheuring B, Ahrendt H, Hunziker JC, Zingg A (1974) Paleobotanical and geochronological evidence for the Alpine age of the metamorphism in the Sesia Zone. Geol Rundsch 63:305–326

Stöckhert B, Jäger E, Voll G (1986) K–Ar age determinations on phengites from the internal part of the Sesia Zone, Western Alps, Italy. Contrib Mineral Petrol 92:456–470

Tilton GR, Schreyer W, Schertl H-P (1991) Pb–Sr–Nd isotopic behaviour of deeply subducted crustal rocks from the Dora Maira massif, western Alps, Italy. II. What is the age of the ultrahigh-pressure metamorphism? Contrib Mineral Petrol 108:22–33

Venturini G, Martinotti G, Hunziker JC (1991) The protoliths of the "Eclogitic Micaschists" in the Lower Aosta Valley (Sesia-Lanzo Zone, Western Alps). Mem Sci Geol Padova 43:347–359

Venturini G, Martinotti G, Armando G, Barbero M, Hunziker JC (1994) The Central Sesia-Lanzo Zone (Western Italian Alps): new field observations and lithostratigraphic subdivisions. Schweiz Mineral Petrogr Mitt 74:115–125

Williams PF, Compagnoni R (1983) Deformation and metamorphism in the Bard area of the Sesia-Lanzo Zone, Western Alps, during subduction and uplift. J Metamorphic Geol 1:117–140